Membrane stability under electrical stress: A nonlocal electroelastic treatment

Michael B. Partenskii, Vladimir L. Dorman, and Peter C. Jordan
Department of Chemistry, Brandeis University, Waltham, Massachusetts 02254

(Received 22 June 1998; accepted 14 September 1998)

Existing models of membrane instability and breakdown under an applied voltage are critically examined. An alternative, speculative treatment of the electroelastic model is suggested, based on the assumption that spatial dispersion of the elastic moduli leads to their effective softening at short wave lengths. The model parameters that account for these effects are chosen to ensure that short wave length thickness fluctuations become unstable at moderate applied voltages, ~1–1.5 V. With these parameters we treat the membrane stretching diagram and membrane thickness fluctuations. The stretching diagram agrees with experimental findings and earlier calculations. Computed thickness fluctuations are consistent with previous investigations. © *1998 American Institute of Physics.* [S0021-9606(98)50847-1]

I. INTRODUCTION

The way that membranes interact with electric fields (applied voltages) and the consequences for membrane stability and electroporation are both very important for the electrical manipulation of membrane behavior.[1–3] By adjusting these fields it is possible to influence transmembrane permeability and thus gain some control over processes such as targeted drug delivery, DNA transport into cells, etc.[4,5] Membrane–field interaction and membrane stability are also crucial for the development of ''bioelectrochemical'' sensors where membranes are in contact with electrodes and an applied voltage is used for monitoring changes caused by their interaction with the environment.[6–10] Study of the influence of solid supports (electrodes) on membrane stability is important both for the development of this field and in order to provide improved insight into the mechanisms of membrane breakdown.

Understanding the mechanisms of membrane breakdown under an applied voltage can also lead to improved understanding of related phenomena, such as transport of neutral molecules and ions across the membrane, formation of hydrophobic pores and proton wires, membrane fusion, stability of patch clamps, etc. It may also have consequences for protein insertion, the stability of peptide assembles in membranes, the translocation of segments during channel formation, etc.

Notwithstanding the intensive experimental and theoretical study of membrane electrical breakdown that has occurred during the last 20 years (see Refs. 2, 11), the mechanism of rupture and in particular, any precursor membrane instability is still not satisfactorily understood. The first electroelastic model of these phenomena, suggested by Crowley[12] predicts significant membrane thinning at the critical point and a critical voltage V_{cr} far exceeding experimental values. More recent work has focused on pore formation as the mechanism for the development and propagation of the instabilities that lead to rupture (see Weaver and Chizmadzhev[13] for a topical overview of the field). This mechanism postulates that initiation of instability occurs via large fluctuations leading to the formation of hydrophobic pores.[14] While this model's analysis of the growth and development of pores, once formed, seems well established,[2,15–17] there is less certainty in its description of the initial step in pore formation. Our analysis focuses on a possible mechanism for introducing the instability required for pore nucleation.

An alternative description of membrane stability has been based on a hydrodynamic model, originally developed for liquid films in contact with various media.[18–20] Subsequently this approach was extended to viscoelastic films designed to imitate membranes (see Refs. 11,21,22, and references therein). The formation of the pores and film rupture arose due to instability of the symmetric ''squeezing modes'' (SQM) related to the thickness fluctuations [distinct from the antisymmetric ''bending modes'' (BM), which may sometimes be associated with ''buckling'' instability[11]]. A number of studies[11,23–26] concluded that the SQM could be unstable at small voltages with low associated thinning, consistent with those experimental results.

However, as has been shown[21,22,27–29] these analyses did not account for the elastic force normal to the membrane plane which opposes thickness fluctuations; consequently, these studies also implied that the threshold voltage for breakdown is zero[23] if surface tension vanishes. Thus, the approach is more appropriate for liquid systems, where thickness fluctuations arise from redistribution of molecules between surface and inner regions of the film. In addition to simple liquids, this model is also descriptive of ''colored lipid films.''[30,31] But it is less appropriate for lipid bilayers, where thickness variation measures the change in distances between lipid head groups on opposite sides of the membrane, and where steric interaction between the hydrocarbon tails in the midplane of the bilayer provides a quasielastic force opposing those fluctuations, a force which stabilizes the bilayer. If the viscoelastic model is modified to account

for this force, the original Crowley model problems recur; breakdown requires extensive thinning.[32]

We base our analysis on the smectic bilayer model of the membrane. In this model small deformations of the membrane surface lead to the appearance of quasielastic (restoring) forces described by two basic moduli (''stretching'' and ''bending''), and by surface tension. Models of this type have been successfully used to describe the stretching diagrams and adhesion[33] of membranes, peptide insertion into membranes,[34,35] the spectrum of surface undulations,[36] etc. In this paper we focus on criteria for instability. In this sense our treatment does not differ from that of a properly formulated viscoelastic model. This is because the transition from a stable to an unstable regime is effected through a motionless state of neutral stability.[22] In this regime, viscous contributions are negligible. For subsequent work, where the relaxation from stable to unstable states is to be studied, inclusion of viscoelastic effects is necessary.

In its original form the smectic bilayer approach yields results very similar to Crowley's original predictions. Therefore we modify the model and introduce an additional assumption, that membrane elastic properties become substantially nonlocal at short wavelengths λ, in analogy to the nonlocality observed for elastic moduli and for dielectric properties of many substances. We show that this hypothesis naturally enhances the electroelastic model of membrane instability; it can rationalize the crucial observations of comparatively low values for V_{cr} associated with only minor membrane thinning. At the same time it predicts significant softening of the symmetric mode of membrane oscillation. Since the local approximation accounts for many equilibrium membrane properties, we then apply the nonlocal formulation to show that it can be similarly successful. We show that the membrane stretching diagram is in accord with experimental findings and the results of earlier calculations and that membrane thickness fluctuations are consistent with results of previous investigations. Some preliminary results have appeared previously.[37,38]

II. SMECTIC BILAYER MODEL IN AN ELECTRIC FIELD

A. Peristaltic and bending fluctuation modes

To analyze membrane stability we generalize the smectic model of a membrane bilayer. Diverse aspects of a smectic description of membrane properties have been studied by different investigators.[34,35,39,40] The total energy contains both an elastic and an electric component. To discuss them we introduce the displacements of the upper (+) and lower (−) membrane surfaces. The corresponding z-components of displacements normal to the membrane midplane XY are $U^+(\boldsymbol{\rho})$ and $U^-(\boldsymbol{\rho})$, with $\boldsymbol{\rho}$ a two-dimensional radius vector in the XY plane. We express these as

$$U^{\pm}=u_0+u^{\pm}, \tag{1}$$

where u_0 is the displacement caused by external forces (such as electric or mechanical stress) while $u^{\pm}$ describes a nonuniform fluctuation of the membrane surface. As long as fluctuations are small the modes can be treated separately. Thus, for further analysis we decompose the $u^{\pm}$ into Fourier series,

$$u^{\pm}(\boldsymbol{\rho})=\sum_q u^{\pm}(\mathbf{q})\exp(\mathbf{iq}\cdot\boldsymbol{\rho}). \tag{2}$$

We now treat separately the peristaltic (symmetric, *s*-) and bending (antisymmetric, *a*-) modes of membrane fluctuations,[20]

$$u_s^+=-u_s^-=u, \tag{3a}$$

$$u_a^+=u_a^-=u. \tag{3b}$$

The elastic energy (per unit area) in the smectic model consists of three contributions:[34,35,40]

(1) *Compression (stretching) energy*, w_1, expressed in a form implicit in the electroelastic model of membrane breakdown (omitting an insignificant constant),[12]

$$w_1=Bh_0z[\ln(z)-1]=Ez[\ln(z)-1], \tag{4}$$

where $z=h/h_0$; $h=h(\rho)$ is the local thickness of the membrane, h_0 its unperturbed value, B and $E=Bh_0$ are the Young's and ''stretching'' moduli, respectively.

(2) *Splay (bending or curvature) energy*, w_2, defined by a splay constant K_1 or by the corresponding elastic modulus $K_c=K_1h^2$,[34]

$$w_2=\frac{K_c}{2}(\boldsymbol{\nabla}_\perp^2u)^2, \tag{5}$$

where $\nabla_\perp\equiv\partial/\partial\boldsymbol{\rho}$ is the gradient operator in the plane of the membrane.

(3) *Surface tension contribution* defined by a stress σ applied to the membrane and typically expressed as[41]

$$w_3=\sigma(\nabla_\perp u)^2/2. \tag{6}$$

Later we will specify separate forms for the last two contributions for both *s*- and *a*-modes.

The electrostatic contribution can be found from the Poisson equation. Neglecting contributions due to the diffuse ionic distribution surrounding the membrane, the membrane surface may be considered an equipotential; the applicability of this approximation is discussed in detail in Appendix A. Then the electrostatic contributions can be found as[20,40,42]

$$w_{el}=-2q|u_q|^2p_E\begin{cases}\tanh(qh/2) & (a\text{-mode})\\ \coth(qh/2) & (s\text{-mode})\end{cases}, \tag{7}$$

$$p_E(V,h)=\frac{\epsilon V^2}{8\pi h^2}, \tag{8}$$

where $p_E(V,h)$ is the electric pressure as a function of applied voltage, V, and membrane thickness, h, and ϵ is the membrane dielectric constant. The equilibrium membrane thickness, $\bar{h}$,

$$\bar{h}=h_0-2u_0, \tag{9}$$

which accounts for electrostriction, is determined from the equilibrium condition

$$\frac{\partial W_0}{\partial \bar{h}} = 0, \tag{10}$$

where W_0 is the energy of the uniform membrane under electric stress,

$$W_0 = E\alpha[\ln(\alpha) - 1] - \epsilon \frac{V^2}{8\pi \bar{h}} \tag{11}$$

and the thinning coefficient $\alpha = \bar{h}/h_0$. Then it follows that at equilibrium

$$E\ \ln(\alpha) = -p_E h_0, \tag{12}$$

which yields the following relation between the applied voltage (in volts) and α;[43]

$$V = 300\alpha \sqrt{\frac{8\pi E h_0}{\epsilon} \ln\left(\frac{1}{\alpha}\right)}. \tag{13}$$

Using Eqs. (1) and (9) we have

$$h(\rho) = \bar{h} + u^+ - u^-. \tag{14}$$

The fluctuating ($\sim u^2$) part of the compression energy is

$$w_1^{(2)} = \frac{1}{2} \left.\frac{\partial^2 w_1(z)}{\partial z^2}\right|_{z=\alpha} (z-\alpha)^2 = \frac{E}{2h_0^2\alpha} (u^+ - u^-)^2. \tag{15}$$

Summing up the contributions of Eqs. (5)–(7) and (15) we can express the energies of the *s*- and *a*-modes (w_s and w_a) as

$$w_{s,a} = 2 \frac{E|u_q|^2}{h_0^2} f_{s,a}(x,\alpha), \tag{16}$$

$$f_s(x,\alpha) = \frac{1}{\alpha} + b_1 \gamma x^2 + b_2 \xi x^4 + x\ \ln(\alpha) \coth\left(\frac{x\alpha}{2}\right), \tag{17}$$

$$f_a(x,\alpha) = \gamma x^2 + \xi x^4 + x\ \ln(\alpha) \tanh\left(\frac{x\alpha}{2}\right), \tag{18}$$

where

$$\xi = \frac{K_c}{4Eh_0^2}, \quad \gamma = \frac{\sigma}{4E}, \quad x = q h_0. \tag{19}$$

The dimensionless constants b_1 and b_2 were introduced by Leikin;[40] they account for the fact that contributions from each monolayer to the bending modulus and the surface tension can differ for the two modes considered. Such effects are probably small so that $b_1 \sim b_2 \sim 1$.[40] Finally, it should be noted that the electric potential enters Eqs. (11) and (16) only through the parameter α describing the uniform compression of the membrane by the applied voltage.

B. Instability of the BM under an applied voltage

Without an applied stress bending modes are unstable at most applied voltages in the long λ limit (small x). To illustrate this, note that $x \tanh(\alpha x/2) \sim \alpha x^2/2 - \alpha^3 x^4/24$ as $x \to 0$; in this limit Eq. (18) yields

$$f_a(x,\alpha) \sim x^2(\gamma + \alpha\ \ln(\alpha)/2) + x^4(\xi - \alpha^3\ \ln(\alpha)/24). \tag{20}$$

TABLE I. Elastic parameters for representative soft and rigid membranes (see text).

Membrane	E (dyn/cm)	h_0 (Å)	K_c (erg)	ξ [Eq. (19)]
SOPC[a]	200	28	0.9×10^{-12}	0.014
SOPC:CHOL[b]	600	34	2.4×10^{-12}	0.0087

[a]References 44–46.
[b]Reference 45.

The lower bound to x, $x_{\min}$, corresponds to $\lambda = \lambda_{\max} = L$ and $x_{\min} = 2\pi h_0/L$. As long as L is substantially larger than h_0, $x_{\min} \ll 1$ and the second term in Eq. (20) can be neglected, long λ stability is determined by γ and V. The bending mode is stable if

$$\gamma + \tfrac{1}{2}\alpha\ \ln(\alpha) > 0. \tag{21}$$

For the physically interesting region, $\alpha \sim 1$ this reduces to $\alpha(1-\alpha) < 2\gamma$ or $\alpha > 1 - 2\gamma$. Since $\gamma = (\sigma/4E) \ll 1$ for reasonable values of σ, we find from Eq. (13) that

$$V < 300 \sqrt{\frac{4\pi\sigma h_0}{\epsilon}}. \tag{22}$$

It follows from Eqs. (21) and (22) that the only stabilizing force at long λ is the membrane tension, and V_{cr} vanishes as $\sigma \to 0$. This instability has been discussed extensively in a number of studies (see Refs. 13,20,27, and references therein).

Assuming that the mechanical tension σ arising from contact of the lipid film with the bulk phase (lenses) is typically $\sigma \leqslant 2$ dyn/cm, choosing $\epsilon = 2$ and using experimental data for representative soft [stearoyloleoylphosphatidylcholine (SOPC)] and rigid (SOPC-cholesterol, SOPC:CHOL) membranes presented in Table I we find in both cases a stability range of $V \leqslant 0.6$ V.

Experimentally, the characteristic critical voltage V_{exper} depends on the duration τ of the applied electric pulse. For brief pulses, ($\tau \sim 0.01 - 0.1$ μs) $V_{exper} \sim 1$ V, and for longer ones ($\tau \sim 1$ μs) $V_{exper} < 0.5$ V.[47] Further increase of τ leads to even smaller V_{exper} [see Ref. 48 for lipid bilayers and Ref. 49 for bilayers with inclusions (fluid mosaic cell membranes), and references therein]. Thus the onset of BM instability is likely related to the long τ pulse observations. The increase of electroporation threshhold[48] with addition of surfactants is also in qualitative agreement with Eq. (22) if the reduction of σ by surfactant is taken into consideration.

C. Instability of the SQM under an applied voltage

Unlike the BM which is unstable if $\sigma \to 0$, the SQM is strongly stabilized by the quasielastic forces due to steric interaction of the hydrocarbon tails of lipid molecules. Therefore a SQM instability generally requires higher voltages than those leading to BM instability.

We now relate the smectic approach to Crowley's model in the limit $x \to 0$. Consider the stability of SQM (*s*-modes). They become absolutely unstable when $f_s(x,\alpha) = 0$. In practice, as a consequence of membrane fluctuations, a transition to a new state occurs before this point is reached, (see the corresponding discussion for elastic capacitor models[50]).

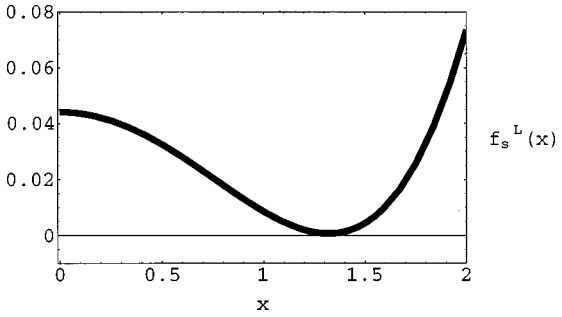

FIG. 1. Local (dimensionless) energy of *s*-mode fluctuations.

First we consider the small x (long wavelength, $\lambda = 2\pi/q$) limit where $x\coth(x) \sim 1$ and all contributions to Eqs. (16) and (17) of higher order in x are neglected. The corresponding condition, $2\ln(\alpha) = -1$, is exactly Crowley's original result,[12]

$$\alpha_{\mathrm{Crow}} = 1/\sqrt{e} = 0.60653. \tag{23}$$

This corresponds to the loss of stability for a membrane uniformly compressed by an applied voltage; the result follows from the general conditions for critical behavior, that W_0 simultaneously satisfy Eq. (10) and the curvature condition

$$\frac{\partial^2 W_0}{\partial \overline{h}^2} = 0. \tag{24}$$

Equation (23) illustrates a major shortcoming of the original electroelastic model; it predicts membrane thinning of almost 40%, a result vastly different from the experimental finding that $\alpha \gtrsim 0.97$.[51] The corresponding critical voltage V_{Crow} can be determined from Eq. (13). Thus, for SOPC, with data from Table I, we find $V_{\mathrm{Crow}} \sim 3.4$ V (Ref. 52) (see also Ref. 13) so that both the extent of membrane contraction and the breakdown voltage predicted by Crowley's model greatly exceed the experimental values.

We now consider how finite wavelength fluctuations influence *s*-mode stability in the smectic model. The only negative contribution to the energy in Eq. (16) arises from the electrostatic term, $x\ln(\alpha)\coth(x\alpha/2)$ in Eq. (17). Its absolute value is essentially a linearly increasing function for $x \gtrsim 0.5$. One can thus expect that the instability criteria at finite x will be softer than for a uniform contraction corresponding to $x = 0$. And this is the case. But, because of rapid ($\sim x^4$) growth of the positive bending energy term, the instability still occurs at a fairly small value of x (roughly $\lambda \sim 6h_0$, i.e., $x \sim 1$); the corresponding values of α_c and V_c remain very close to the Crowley result. Analysis of experimental data, like those of Table I, indicates that typical values of the dimensionless bending constant ξ, Eq (19), fall in the range between 0.008 and 0.02. In Fig. 1 we present the dimensionless energy of the *s*-mode, $f_s(\alpha, x)$, for SOPC and $\alpha_c \sim 0.615$, the conditions under which this mode becomes unstable. As is apparent, this occurs at finite x (~ 1.25), before the Crowley condition is reached ($\alpha > \alpha_{\mathrm{Crowley}}$) so that $f_s(\alpha_c, x = 0) > 0$. Unfortunately, this softening of the instability criteria is too small (the change in V_c does not exceed 2 to 5 mV) to have any practical implications. Consequently, simple electroelastic theory, even when extended to treat short wavelength excitations, cannot account for the observation that the instabilities occur at low transmembrane voltage and with little associated electrostriction.

III. NONLOCAL MODEL OF MEMBRANE INSTABILITY

It follows from the previous discussion that the electrostatic contribution grows in absolute value with x (with decreasing fluctuation wavelength λ). But the influence of a nonuniform electric force in creating an instability is overwhelmed by the stabilizing bending contribution. As a result, the instability is shifted to finite x (~ 1.25) but the corresponding critical voltage remains large (not differing noticeably from the Crowley result) and so does the associated membrane electrostriction. At small voltages (corresponding to $\alpha \geqslant 0.9$) the influence of the electric field on *s*-type fluctuations in the smectic bilayer model is negligible. Therefore this model can not explain how small transmembrane voltages can lead to membrane breakdown. This difficulty has stimulated an alternative approach to modeling breakdown. Instead of studying the stability of small (linear) membrane thickness fluctuations, this approach focuses on large fluctuations leading to formation of transmembrane pores (see Ref. 13, and references therein). The initial stage of the breakdown in this model is associated with the formation of hydrophobic pores (HP), single files of water molecules interposed between the hydrocarbon tails of lipid molecules.[14] Nucleation of a HP requires cooperative motion of ~ 8 lipid molecules and 8–10 water molecules. Given that the lipid molecules are not rigid, the associated kinetic problem is hard to quantify with precision.[15,16] Estimates of the frequency factor, ν, for this process are very approximate and vary over 9–10 orders of magnitude; correspondingly, estimates of the associated energy barrier vary from 30 to 50 kT and pore concentration estimates are not reliably based.[53]

We propose that the initial stage of pore formation arises due to thickness fluctuations destabilized by the electric field. To make this mechanism effective, we assume that at short wavelengths membrane elastic properties differ significantly from their long λ behavior. In the previous analysis we used elastic moduli derived, e.g., from the experiments on shape fluctuations of vesicles,[36] with characteristic wavelengths typically $\geqslant 1$ μm.

We assume that at much shorter wavelengths, comparable to the membrane width, elastic moduli become substantially nonlocal and *s*-modes with corresponding q become ''softer.'' This increases the corresponding fluctuations and makes them more responsive to the action of an applied voltage. This assumption is based on the analogies to dielectric and elastic behavior. It is known that spatial dispersion of the dielectric constant $\epsilon(q)$ leads to substantially lower (and even negative) values of ϵ at short wavelengths,[54,55] and that there is significant spatial dispersion in elastic moduli of ordered materials.[56] Aspects of short wavelength behavior in smectic liquid crystal phases have been modeled by assuming that either (or both) the compression and splay moduli exhibit notable wave vector dependence.[57–59]

There are numerous ways to model this effect. We could reformulate the underlying constitutive equations describing

elastic behavior in coordinate space to incorporate nonlocality. Instead, we build on the formulation of Eq. (17) and carry out our analysis in Fourier space. While the approaches are equivalent, extension of the electroelastic model lends itself more easily to *q*-space treatment. We discuss this point in Appendix B.

We introduce a ''switching function'' $t(x)$, which changes the ''macroscopic'' expressions, Eqs. (16)–(18), for the elastic energy to a different functional form in the small λ region, $\lambda \sim (1 \text{ to } 1.5)\, h_0$,

$$t(x) = \frac{\exp(-\beta a)+1}{\exp[-\beta(a-x)]+1}. \tag{25}$$

Here β characterizes the steepness (sharpness) of the transition and a is the characteristic value of x for the transition. We now have to choose a general form for the short-λ behavior of the *s*-mode energy. It is important to notice that for small λ the separation of energy into pure stretching and bending contributions may not make sense; individual moduli lose their initial meaning, and only the overall behavior of the elastic energy is important. We further assume that the membrane tension contribution (w_3) does not change with this transition thus focusing only on the elastic ''self-energy'' of the membrane. We consider two different approximations to the energy in the short λ limit. The corresponding energy dispersion equations are

$$f_{s1}(x,\alpha) = [1-t(x)]^4(k_1+\xi r_1 x^4) + t(x)^4[1/\alpha + \xi x^4 + \gamma x^2 + \ln(\alpha)x\coth(\alpha x/2)], \tag{26}$$

$$f_{s2}(x,\alpha) = [1-t(x)]^4(k_2+r_2 x) + t(x)^4[1/\alpha + \xi x^4 + \gamma x^2 + \ln(\alpha)x\coth(\alpha x/2)]. \tag{27}$$

At small x, $t(x)\to 1$ and both expressions reduce to Eq. (17). As x increases, $f_{s1}(x,\alpha)$ derives its short-λ structure from that of the long-λ form; it has the same x-dependence, only the moduli are different. The expression for $f_{s2}(x,\alpha)$ accounts for the possibility that the x-dependence in the short-λ limit can be different; we test a linear approximation. The exponent 4 in the expressions involving the switching function $t(x)$ was chosen for mathematical convenience in numerical calculations of the stretching diagram (see below).

For each of the models we have assigned the parameters k_i and r_i characterizing the low-λ limit to yield a voltage-induced instability of the symmetric mode at the expected values of applied voltage $V = V_{cr}$. In fact, V enters the mode energy through the parameter α describing the transverse contraction of the membrane. Given that membrane thinning does not exceed 3%, we chose model parameters so that the *s*-mode energy approaches 0 as $\alpha \to 0.97$. Using Eq. (13) the critical voltage is

$$V_{cr} \sim 254\sqrt{\frac{Eh_0}{\epsilon}}.$$

For SOPC, with data from Table I and $\epsilon \sim 2$, this is ~1.3 V. Figure 2 illustrates how we determine the nonlocal parameters. The thick curves correspond to $V=0$. The values of k_i and r_i are chosen to satisfy the condition that the *s*-mode becomes unstable for $V = V_{cr}$ at $\lambda_{cr} \sim h_0$ (or $x \sim 2\pi$). In other words, we require that $f_s = 0$ when $V = V_{cr}$ and $\lambda = \lambda_{cr}$. The instances where an applied voltage leads to instability are illustrated by thinner curves for both nonlocality models. In this way, using the data from Table I, for SOPC we find that $k_1 \sim k_2 \sim 0.1$, $r_1 \sim 0.06$, and $r_2 \sim 0.02$.

IV. ELASTIC NONLOCALITY AND THE MEMBRANE STRETCHING DIAGRAM

It is well known that surface undulations strongly influence the stretching diagram of membranes. They give rise to nonelastic behavior of the area, $A(\sigma)$, at small tensions σ. In the analysis of these effects symmetric mode contributions to the projected area variation have not traditionally been included, all effects being assigned completely to the bending modes.[39] This has been justified by relative softness of the bending modes, especially in the limit of long λ (small x). However, our assumption of softening of the symmetric modes may enhance their contribution to the projected area at short λ and the dependence of $A(\sigma)$ on stretching. In this section we estimate the significance of this effect. We start with following expression for the variation of the projected area due to undulations[41] (see also discussion below),

$$\Delta A_\perp = -\tfrac{1}{2}A(\mathbf{q}\mathbf{u}(\mathbf{q}))^2. \tag{28}$$

The mean square value of the amplitudes, $u(\mathbf{q})^2$, can be determined using the principle of energy equipartition,

$$A\langle w_{s,a}\rangle = kT/2. \tag{29}$$

Then, using Eqs. (16)–(18) we find

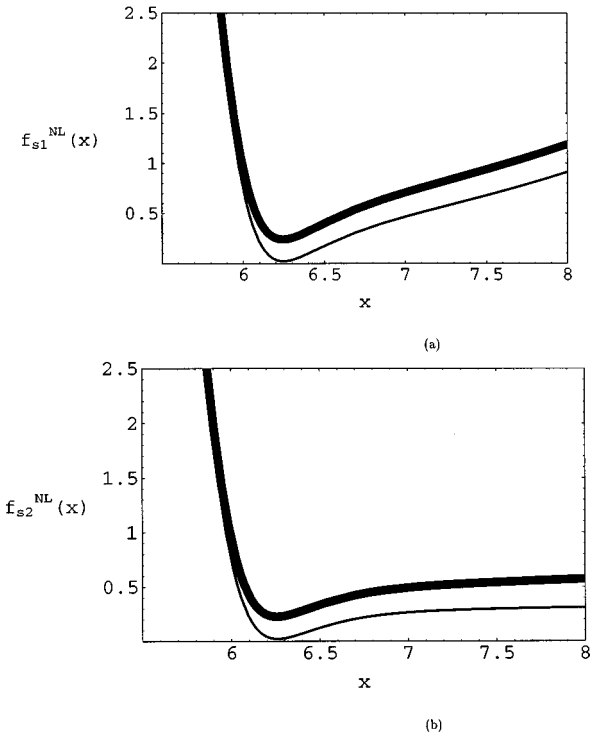

FIG. 2. Nonlocal (dimensionless) energy of the *s*-mode in two approximations for the transitional and short λ regions at $V=0$ ($\alpha=1$, upper curve) and at $V=1.3$ V ($\alpha=0.97$, lower curve) (a) $f_{s1}(x,\alpha)$ and (b) $f_{s2}(x,\alpha)$.

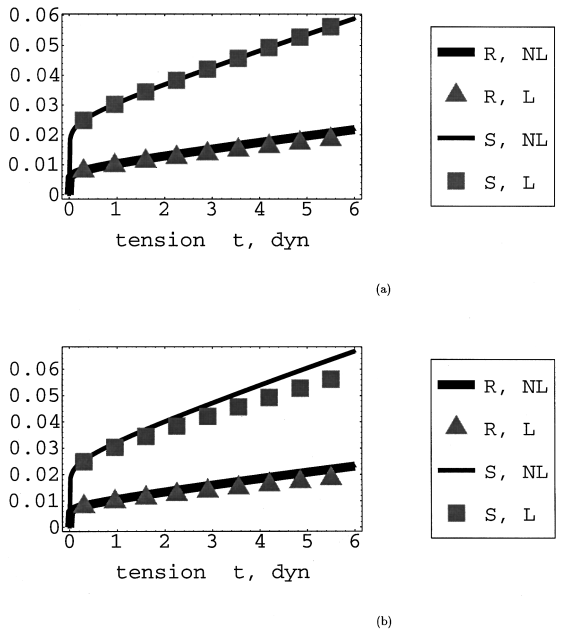

FIG. 3. Stretching diagram for soft (S) and rigid (R) membranes for (a) $\lambda_{min}=15$ Å and (b) $\lambda_{min}=12$ Å. ''L'' corresponds to the local [Eq. (34)] model, while ''NL'' describes the nonlocal calculations with $k_1=0.1$ and $r_1=0.06$ (S) and $k_1=0.1$ and $r_1=0.04$ (R).

$$\langle |u_{s,a}|^2 \rangle = \frac{kTh_0^2}{4AEf_{s,a}(x,\alpha)}, \tag{30}$$

from which we determine

$$\Delta A_{\perp s,a}(q) = -\frac{kTx^2}{8Ef_{s,a}(x,\alpha)}. \tag{31}$$

We now define

$$\nu \equiv \frac{\Delta A_\perp}{A}, \tag{32}$$

the fractional variation of the projected area due to membrane undulations. To find ν we sum up contributions of modes with different $\mathbf{q}$ using

$$\sum_q (\cdots) \rightarrow \frac{A}{2\pi} \int qdq(\cdots).$$

As a result we obtain

$$\nu_{1,2} = \frac{-kT}{16\pi Eh_0^2} \int_{x_{min}}^{x_{max}} x^3 \left(\frac{1}{f_{s1,2}(x,\alpha)} + \frac{1}{f_a(x,\alpha)} \right) dx, \tag{33}$$

where the indices 1 and 2 correspond to the expressions Eqs. (26) and (27) describing the nonlocal dispersion of the symmetric mode. In the local approximation ($t(x)=1$), and neglecting the s-mode contributions these equations reduce exactly to Helfrich's result[41]

$$\nu_{Helf} = -\frac{kT}{32E\pi\xi h_0^2} \log\left(\frac{x_{max}^2 + \gamma/\xi}{x_{min}^2 + \gamma/\xi} \right). \tag{34}$$

We now contrast stretching diagrams calculated in the local (L) and nonlocal (NL) approximations (Fig. 3) using the data from Table I for soft (SOPC) and rigid (SOPC: CHOL) membranes. The nonlocal calculations are based on the first form for the modified dispersion relation, Eq. (26). The results obtained using the alternate form, Eq. (27), to describe the short λ limit are practically the same; the calculated stretching diagrams are basically independent of the way in which mode softening is treated. At small tensions ($\tau \leqslant 0.2$ dyn) the slope of the stretching diagrams is very steep. This domain corresponds to the so-called ''nonelastic'' (entropic) region of membrane stretching. For $\tau \geqslant 3$–4 dyn the slope is practically constant. In the intermediate region there is a sharp transition between these two regimes.

Unlike the local calculations, the nonlocal results depend somewhat on the choice of λ_{min} (or x_{max}). With $\lambda_{min}=15$ Å local and nonlocal diagrams are practically the same [Fig. 3(a)] while for $\lambda_{min}=12$ Å [Fig. 3(b)] there is a noticeable difference for the soft membrane which becomes more pronounced at smaller λ_{min}. Since local theory reproduces experimental stretching diagrams satisfactorily, discussion of the appropriate choice of λ_{min} in nonlocal calculations is required. Consider Eq. (28). Its derivation assumes that the total membrane area is fixed. Undulations only change the projected area. This requires that the lipid head groups tend to be oriented similarly with respect to the local interface, an assumption certainly valid for long λ where the interface is locally flat; then local conditions are the same as for the plane membrane. However, this relation changes at shorter wavelengths. For $\lambda \sim 15$–20 Å the relative displacements of the neighboring head groups are $\sim u$ in which case the up- and down-types of displacement are the natural ones, motions that conserve the projected area. In other words, Eq. (28) should be modified to account for the short λ dispersion of the projected area. We account for this by simply applying a cutoff on λ. The value $\lambda \sim 15$–20 Å, as outlined above, is a reasonable limit for validity of the macroscopic expression, Eq. (28).

V. MEMBRANE THICKNESS FLUCTUATIONS

Membrane thickness fluctuations have been studied by Hladky and Gruen (HG).[60] Their original goal was to determine if thermal fluctuations might account for literature reports of differences between the mean ''electrical'' (as determined by capacitance measurements) and ''optical'' (as determined by optical reflectance studies) membrane thickness. Later studies showed these differences to be chimerical[61] but it is still of interest to determine whether two very different models of membrane behavior lead to similar conclusions. HG treat a reduced version[18,62] of the smectic model of section 2 which ignores splay [$\xi=0$ in Eqs. (17) and (18)] and assumes that the membrane can be described by an inherent surface tension σ in Eq. (6) [or equivalently γ in Eqs. (17) and (18)].[63] This stress can be created either by mechanical means (e.g., osmotic stress), or by contact between the bilayer and a bulk lipid phase, due to a difference between the chemical potential of lipid in bulk and in the bilayer. We wish to show that, just as for the stretching diagram, the non-local model yields similar predictions. As thickness fluctuations have not been directly measured, we only seek qualitative agreement between our analysis and that of HG.

TABLE II. Thickness fluctuations ($\Delta\tilde{h}$, in Å) for (*S*)oft and (*R*)igid membranes for different membrane models (see text).

λ_{min}(Å)	*S*, *L*	*S*, NL	*S*, HG[a]	*R*, *L*	*R*, NL	*R*, HG[a]
10	1.60	3.28	6.6	0.90	1.77	5.1
100	0.4	0.4	0.8	0.2	0.2	0.6

[a]Fluctuations computed using the HG approach (Ref. 60).

The thickness fluctuations can be analyzed in a manner similar to that used in determining the membrane stretching diagrams. It follows from Eq. (14) that at small electric fields (where $u_0 \sim 0$) $h(\rho)=h_0+2u_s(\rho)$. Then, using the Fourier decomposition Eq. (2), we find

$$\langle (h-h_0)^2 \rangle = 4\sum_{\mathbf{q}} |u_s(\mathbf{q})|^2, \tag{35}$$

with which, proceeding as in Eqs. (29)–(33), we obtain

$$\langle (h-h_0)^2 \rangle = \frac{kT}{2\pi E} \int_{x_{min}}^{x_{max}} \frac{x}{f_s(x,\alpha)}\, dx. \tag{36}$$

Following HG we contrast results for two wavelength (λ) cutoffs, $\lambda_{min}=10$ Å and $\lambda_{min}=100$ Å; λ_{min} corresponds to the upper limit of the integral in Eq. (36) since $x_{max}=2\pi h_0/\lambda_{min}$. The lower limit, x_{min} depends on the characteristic size of the membrane; in practice it can be set equal to 0. Defining rms thickness fluctuations, $\Delta\tilde{h} \equiv \langle (h-h_0)^2 \rangle^{1/2}$, our results for SOPC (soft) and SOPC:CHOL (rigid) membranes are presented in Table II and compared with values computed using the HG approach for two different λ cutoffs.

Thickness fluctuations in our theory are comparable in magnitude, but slightly smaller, than those found by HG. Regardless of membrane stiffness, the variation of $\Delta\tilde{h}$ with cutoff λ is the same for the nonlocal and the HG approaches; however, our analysis predicts that the fluctuations are 2–3 times smaller. The local approximation predicts that $\Delta\tilde{h}$ is far less sensitive to the choice of cutoff λ. The qualitative agreement between two physically very different descriptions of membranes behavior is surprisingly good. From Eq. (36) thickness fluctuations are inversely proportional to mode energy. In our theory the large x contribution arises mainly from nonlocality (in the local limit the x dependence is much smaller), while in HG this difference is mainly due to a much more gradual (x^2) increase of the mode energy (as compared with an x^4 dependence in our local smectic bilayer model).

The general picture is that, when compared with the HG study, nonlocality, and mode softening do not lead to dramatic changes in mean membrane thickness fluctuations. However, for a nonlocal membrane, the fluctuation spectrum should peak at wavelengths ~30–50 Å. Thus a valuable test of our model would come from investigating this range of thickness fluctuations, either by means of molecular dynamics simulations or directly, by soft x-ray scattering from real membranes.

VI. SUMMARY AND DISCUSSION

We have reconsidered the electroelastic model for membrane breakdown. In order to circumvent its well-known limitations (membranes are incorrectly predicted to undergo rupture at high voltages, ~4 V, with significant electrostriction, ~40%) we have considered whether the origin of breakdown (and the subsequent electroporation) may be due to nonlocality of a membrane's elastic moduli and their softening at short wavelength. With this assumption we find that instability of membrane thickness fluctuations is possible at fairly low voltages (~1 V) with negligible electrostriction. To demonstrate the feasibility of this idea we have (1) computed the membrane stretching diagram and shown that the nonlocal model reproduces results of traditional theories; (2) investigated thickness fluctuations and shown that our analysis is consistent with the results of previous theoretical treatments.

Although partially hidden in averaged thermodynamic properties like the stretching diagram, nonlocality may play a very important role when the influence of short-scale perturbations of the membrane surface is significant. One example is membrane breakdown under an applied voltage, where the electric field interacts strongly with short-λ fluctuations. Nonlocality can also have a direct relation to the anomalous roughness of a membrane surface[33] suggested to explain the discrepancy between calculations of adhesion energy based on the Young equation and on the conventional (local) theory of the entropic forces between the membranes. Mode softening could be a reason for this roughness and for the corresponding hidden projected area,[33] a suggestion complimentary to the hypothesis of special types of structural defects (hats and saddles).[64] It may also be related to the finding of ''remarkable out-of-plane vibrational motion'' of lipid molecules[65] which can contribute strongly to short-range repulsive forces between membranes.[66] We plan to pursue these issues in forthcoming studies.

Further development of the nonlocal model should account for factors not considered here. For instance, it is natural to assume that at sufficiently high tensions, comparable to critical values, the softening of short-λ moduli would be noticeably tension dependent. This provides a further avenue for analyzing the combined effect of mechanical and electric stresses on membrane breakdown. The effects of surfactants and the influence of solid supports are other areas for future studies.

Possible ways to directly observe and analyze nonlocal effects must be considered. One important way to study nonlocal influences on membrane fluctuations could be molecular dynamics modeling. A possible difficulty with such analysis should be mentioned. In its natural environment the membrane assumes a stressless state. However, MD modeling requires imposition of specific boundary conditions, ones which correspond to a stressed state of membrane (see Refs. 67–69 for discussion). This stress can interfere with the fluctuations of membrane shape and thickness, an effect that must to be accounted for in analyzing data extracted from computer experiments.

Two different types of instability can possibly contribute to membrane breakdown. The first is the bending mode in-

stability, known to occur at long wavelengths and small voltages. As discussed in Sec. II B this BM instability can be related to long pulse perturbations. The SQM instability occurs at short λ and can be related to short pulse experiments. Our current analysis only touches the issue of instability onset, not the kinetics of its growth leading either to formation of pores or to the creation of intermediate nonuniform phases.[50] To describe kinetics, the dynamic equations for some reasonable viscoelastic membrane model must be solved. As discussed in Sec. I, there is still disagreement as to the proper way to account for elastic effects in such a model. Accounting for nonlocality will provide a further challenge in solving this problem.

ACKNOWLEDGMENT

This work was supported by Grant No. GM-28643 from the National Institute of Health.

APPENDIX A

In the metallic approximation used in the bulk of this paper, the potential difference V between the membrane surfaces is assumed to be fixed. In fact only the potential drop between the bulk electrolytes separated by the membrane can be controlled, the actual potential drop across the membrane being dependent on the screening properties of the solvents. Consequently, the influence of the electrostatics on membrane oscillations differs from its metallic limit. To determine the importance of electrolyte screening we apply the Poisson–Boltzmann theory.[70] Limiting analysis to a single one-dimensional symmetrical surface deformation of wave number q, the interface, z_0, between the electrolyte and a membrane of equilibrium thickness h can be expressed as

$$z_0(y)=h/2+u_q\cos qy, \tag{A1}$$

where u_q is the amplitude of the surface fluctuation. The system is governed by Poisson's equation in the membrane and the Poisson–Boltzmann equation in the electrolyte,

$$\nabla^2\psi=0, \quad \text{membrane}, \tag{A2}$$

$$\nabla^2\psi=\kappa^2\sinh(\psi-W_0), \quad \text{electrolyte}, \tag{A3}$$

where ψ is the dimensionless electrical potential, $e_0\phi/k_BT$, κ is the reciprocal of the Debye length, and W_0 is half the dimensionless applied voltage, $e_0V/2k_BT$. The total electrostatic energy of the open (when V is fixed) system is

$$U_{\text{Field}}=-\frac{1}{8\pi}\int dV\mathbf{D}\cdot\mathbf{E}, \tag{A4}$$

where $\mathbf{E}$ and $\mathbf{D}\equiv\epsilon\mathbf{E}$ are the electric field and electric displacement, respectively, and ϵ is the dielectric constant.

We linearize Eq. (A3) (most of the potential drop takes place across the membrane), $\psi-W_0\ll 1$, and consider small amplitude surface fluctuations, $u_q\ll h$. As the electrical energy, Eq. (A4), is a quadratic function of the field strength (and thus of u_q), we must consider overtones in q,

$$\psi=W_0\left(\chi_0(z)+\sum_n\chi_n(z)\cos(nqy)\right); \tag{A5}$$

linearizing Eq. (A3), we find

$$\chi_0=Az, \quad \chi_n=u_qB_n\sinh(nqz) \quad \text{(membrane)}; \tag{A6}$$

$$\chi_0=1-Ce^{-\kappa(z-h/2)}, \quad \chi_n=u_qD_ne^{-\gamma_n(z-h/2)},$$

$$\gamma_n^2=\kappa^2+n^2q^2 \quad \text{(electrolyte)}. \tag{A7}$$

Standard boundary conditions apply; ψ and the normal displacement $\mathbf{D}_{\text{norm}}$ are continuous across the dividing surface, Eq. (A1). From continuity of ψ we obtain

$$Az_0+u_q\sum_n B_n\sinh(nqz_0)\cos(n\omega)$$

$$=1-Ce^{-\kappa u_q\cos\omega}+u_q\sum_n D_ne^{-\gamma_nu_q\cos\omega}\cos(n\omega) \tag{A8}$$

and from continuity in $\mathbf{D}_{\text{norm}}$ we obtain

$$\epsilon_{\text{memb}}\Big(A+qu_q\sum_n B_n\cosh(nqz_0)\cos(n\omega)$$

$$\times[1-qu_q\tanh(nqz_0)\tan(n\omega)\sin\omega]\Big)$$

$$=\epsilon_{\text{bulk}}\Big(C\kappa e^{-\kappa u_q\cos\omega}\sin(n\omega)$$

$$-u_q\sum_n D_ne^{-\gamma_nu_q\cos\omega}\cos(n\omega)$$

$$\times[\gamma_n+q^2u_q\tan(n\omega)\sin\omega]\Big), \tag{A9}$$

where $\omega\equiv qy$ and $z_0(y)$ is given by Eq. (A1). Substituting Eqs. (A5), (A6), and (A7) into Eq. (A4), expressing W_0 in terms of V, and keeping only terms up to $O(u_q^2)$, yields

$$U^*_{\text{Field}}=-\frac{V^2\epsilon_{\text{memb}}}{16\pi}\left(hA^2/2+qu_q^2AB_1\cosh(qh/2)+\frac{qu_q^2}{4}\sum_n nB_n^2\sinh(nqh)\right)$$

$$-\frac{V^2\epsilon_{\text{bulk}}}{16\pi}\left(\frac{\kappa C^2}{2}(1+\kappa^2u_q^2)+\kappa u_q^2\gamma_1CD_1+\frac{u_q^2}{4}\sum_n\frac{D_n^2}{\gamma_n}(\gamma_n^2+n^2q^2)\right). \tag{A10}$$

where U^*_{Field} is the electrostatic energy per unit projected area of the membrane; the quadratic dependence of U^*_{Field} on V, true to all orders of u_q, arises from linearizing the Poisson–Boltzmann equation. Surface deformations influence the uniform solution terms, A and C; using Eq. (A1) and writing Eq.

(A8) as a Fourier expansion in $\cos(nqy)=\cos n\omega$ we find from the $n=0$ term,

$$Ah/2+(u_q/2)\sum_n B_n(e^{nqh/2}I_n(nqu_q)-e^{-nqh/2}I_n(-nqu_q))$$

$$=1-CI_0(-\kappa u_q)+u_q\sum_n D_nI_n(-\gamma_n u_q), \tag{A11}$$

where I_n is the imaginary Bessel function of order n. Similar, but more complex relations can be found for $n>0$ and when satisfying Eq. (A9). For a displacement at wave number q, both B_1 and D_1 are ~ 1, while for $n\geqslant 2$ both B_n and D_n are $\sim u_q$; the latter terms thus contribute to quartic and higher terms in U^*_{Field} and can be neglected. A and C are quadratic in u_q; the leading terms are

$$A=a_0+u_q^2a_2, \quad C=c_0+u_q^2c_2. \tag{A12}$$

With these and the continuity conditions Eqs. (A8) and (A9) we finally obtain

$$a_0=\frac{2}{h(1+\xi)}, \quad c_0=\frac{\xi}{1+\xi}, \tag{A13}$$

$$B_1^*=\frac{\gamma_1(1-r)-\kappa}{\Delta}\,a_0,$$

$$D_1=\frac{-\kappa\,\tanh(qh/2)/q+(1-1/r)}{\Delta}\,a_0, \tag{A14}$$

$$a_2=\frac{(\kappa-\gamma_1)D_1-B_1^*}{h(1+\xi)},$$

$$c_2=-\frac{c_0\kappa^2}{4}-\frac{\xi B_1^*+D_1(\xi\gamma_1+\kappa)}{2(1+\xi)}, \tag{A15}$$

where

$$r=\epsilon_{\text{bulk}}/\epsilon_{\text{memb}}, \quad \xi=2/(\kappa hr), \tag{A16}$$

$$\Delta=1+\gamma_1 r\,\tanh(qh/2)/q, \tag{A17}$$

$$B_1^*\equiv qB_1\,\cosh(qh/2), \tag{A18}$$

and Eq. (A10) becomes

$$U^*_{\text{Field}}=-\frac{V^2}{16\pi}\,(\epsilon_{\text{memb}}a_0^2h/2+\epsilon_{\text{bulk}}\kappa c_0^2/2)$$

$$-u_q^2\,\frac{V^2\epsilon_{\text{memb}}}{16\pi}\,(a_0a_2h+a_0B_1^*$$

$$+(B_1^*)^2\,\tanh(qh/2)/(2q))$$

$$-u_q^2\,\frac{V^2\epsilon_{\text{bulk}}}{16\pi}\,(\kappa(\kappa^2c_0^2+2c_0c_2)/2$$

$$+\kappa\gamma_1c_0D_1+D_1^2(\gamma_1^2+q^2)/(4\gamma_1)). \tag{A19}$$

A nontrivial limiting case, which confirms our analysis, is the ''metallic'' limit, $\epsilon_{bulk}\to\infty$. U^*_{Field} simplifies enormously [from Eq. (A9) both C and the D_n are $\equiv 0$] and the C and D_1 terms in Eqs. (A13) to (A15) vanish; A and B_1^* become

$$a_0=\frac{2}{h}, \quad B_1^*=\frac{-a_0q}{\tanh(qh/2)}, \quad a_2=\frac{a_0q}{h\,\tanh(qh/2)} \tag{A20}$$

and the expression for U^*_{Field} reduces to

$$U^*_{\text{Field},0}=-\frac{\epsilon_{\text{memb}}V^2}{8\pi h}\left(1+\frac{qu_q^2\,\coth(qh/2)}{h}\right). \tag{A21}$$

The undulatory term in this expression differs from Eqs. (7) and (8) by a factor of 2 because our definition of surface deformation, Eq. (A1), is proportional to $\cos(qy)$ not $\exp(i\mathbf{q}\boldsymbol{\rho})$ as in Eq. (2).

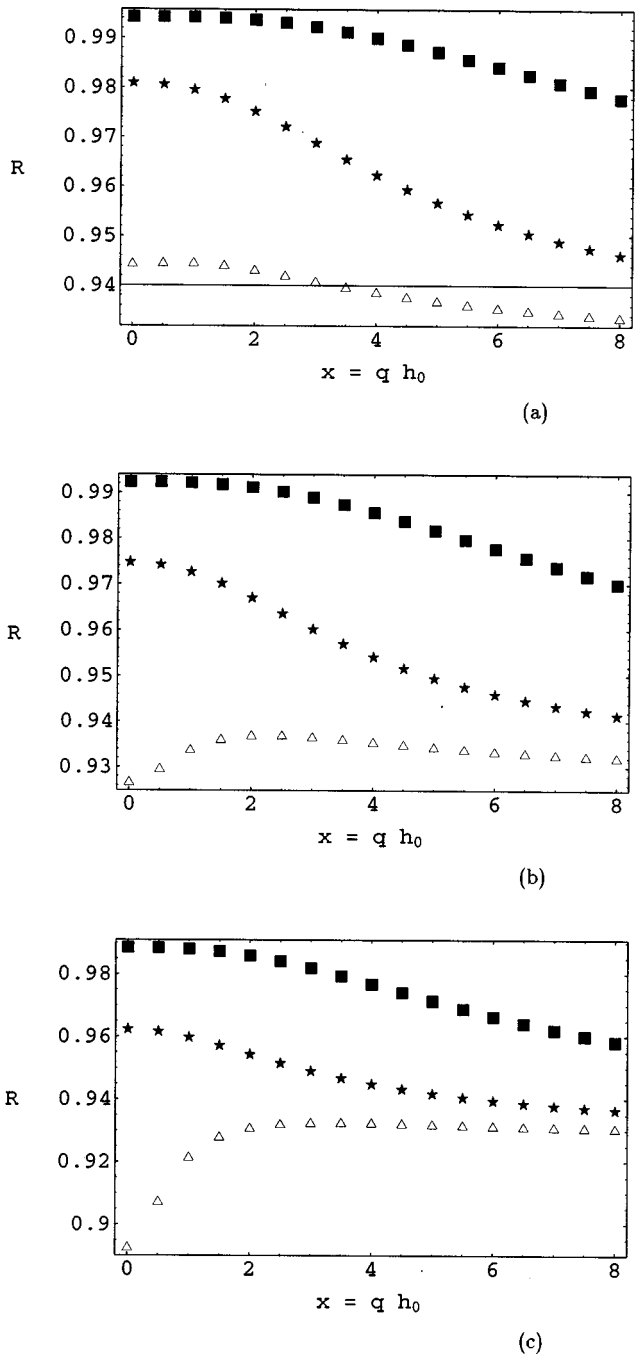

FIG. 4. Ratio R of linear Poisson–Boltzmann calculations of the undulatory part of Eq. (A19) to that in the ''metallic'' limit [Eq. (A21)]. The dielectric ratio r is 40. Three λ_{Debye} values are considered; △, 30 Å; ★, 10 Å; ■, 3 Å. Three membrane thicknesses are contrasted; (a) $h_0=40$ Å, (b) $h_0=30$ Å, (c) $h_0=20$ Å.

Substituting Eq. (A19), in the limit $u_q \to 0$, for the second term in Eq. (11), the total electroelastic energy for the uniform system, including the influence of the diffuse layer, is

$$W_0 = E\alpha[\ln(\alpha) - 1] - \frac{\epsilon_{\text{memb}} r\kappa V^2 (1 + r\kappa h_0 \alpha)^2}{8\pi(2 + r\kappa h_0 \alpha)} \quad \text{(A22)}$$

and the modified form of Eq. (13), relating applied voltage to the thinning coefficient, is

$$V = 300\alpha \left(\frac{2 + r\kappa h_0 \alpha}{r\kappa h_0 \alpha}\right)^{1.5} \sqrt{\frac{8\pi E h_0}{\epsilon_{\text{memb}}} \ln\left(\frac{1}{\alpha}\right)}$$
$$= (1 + \xi)^{1.5} V(\text{metallic}); \quad \text{(A23)}$$

for a typical membrane, with $h_0 \sim 30$ Å, $r = 40$ and $\kappa^{-1} \equiv \lambda_{\text{Debye}}$ between 3 and 30 Å (1 M to 0.01 M ionic strength), the correction factor $(1+\xi)^{1.5}$ is qualitatively insignificant, varying between 1.008 and 1.08. In Fig. 4 we present the ratio of the undulatory term in the electric energy for a membrane sandwiched between realistic electrolytes ($\epsilon_{\text{bulk}} = 80$, $r = 40$) to that in the metallic approximation ($\epsilon_{\text{bulk}} = \infty$, $r = \infty$). Again, ionic strengths (I) ranging from 1 M to 0.01 M (λ_{Debye} from 3 to 30 Å) are contrasted. At all membrane thicknesses considered the high I (low λ_{Debye}) results differ insignificantly over the physically important range of x. Deviations become more important as λ_{Debye} increases, but even at the highest value considered the metallic approximation accounts for more than 90% of the exact result over the whole x-range. This remains true even when an unrealistically thin membrane [$h_0 = 20$ Å, Fig. 4(c)] is modeled. Consequently no serious errors are introduced by using the metallic limit throughout.

APPENDIX B

Nonlocality of constitutive equations means that forces acting at a point $\mathbf{r}$ and conjugate to a fluctuating variable s, depend not only on the value of $s(\mathbf{r})$ at $\mathbf{r}$ but also on its behavior in more distant regions. This leads directly to a two-point integral for the energy W so that (in an harmonic approximation)

$$W = \int K(\mathbf{r},\mathbf{r}') s(\mathbf{r}) s(\mathbf{r}') d\mathbf{r} d\mathbf{r}', \quad \text{(B1)}$$

where, depending on the problem of interest, the kernel $K(\mathbf{r},\mathbf{r}')$ depends on a nonlocal susceptibility or nonlocal modulus.

For example, in nonlocal electrostatics, the role of K is played by $\epsilon(\mathbf{r},\mathbf{r}')$, the nonlocal dielectric constant, while electric field strength, $E(\mathbf{r})$, corresponds to $s(\mathbf{r})$.[54,71,72] In elastic theory K is a dynamical modulus $D(\mathbf{r},\mathbf{r}')$ and s describes displacements $u(\mathbf{r})$.[56,71] The local limit in a uniform system corresponds to $K(\mathbf{r},\mathbf{r}') = K \cdot \delta(\mathbf{r} - \mathbf{r}')$ where $\delta(r)$ is a delta-function in which case $W = K \int s^2(\mathbf{r})(d\mathbf{r})$.

As long as K is a function of $\mathbf{r} - \mathbf{r}'$, the Fourier transform of Eq. (B1) is

$$W = \sum_q K(\mathbf{q}) |s_q|^2, \quad \text{(B2)}$$

where $K(\mathbf{q}) = \int \exp(-i\mathbf{q}\cdot\mathbf{r}) K(\mathbf{r})$. Thus, nonlocality can be either described through the spatial dependence of the generalized susceptibility, $K(\mathbf{r},\mathbf{r}')$, or through the dependence of its Fourier transform on the wave vector $\mathbf{q}$.

Fourier representations are often simpler and more understandable. For instance, the kernel $K(\rho)$ corresponding to the stretching and bending contributions to Eq. (17) is complex,

$$\frac{1}{\alpha}\,\delta(\rho) + 2\xi q_{\max}^3 \cdot \pi h_0^4 \,\frac{(q_{\max}\cdot\rho)^2 - 8}{\rho^3}\, J_3(q_{\max}\cdot\rho)$$

(here J_3 is a third order Bessel function) and it is clearly easier to treat the simpler terms in Eq. (17), its Fourier transform. We chose this approach when proposing short-λ nonlocality. It could equally well be described in terms of spatially dependent elastic moduli resulting in a different dispersion law for the mode energy at large x. Instead of formulating new spatial dependence, we treat the dispersion law directly, postulating a transition from long- to short-λ behavior [see Eqs. (25)–(27)].

[1] T. Tsong, Biophys. J. **41**, 135 (1991).
[2] S. Freeman, M. Wang, and J. Weaver, Biophys. J. **67**, 42 (1994).
[3] *Electromanipulation of Cells*, edited by U. Zimmerman and G. Neil (CRC Press, Boca Raton, 1996).
[4] E. Neumann, A. Sowers, and C. E. Jordan, *Electroporation and Electrofusion in Cell Biology* (Plenum, New York, 1989).
[5] E. Neumann, Bioelectrochem. Bioenerg. **28**, 247 (1992).
[6] H. Tien, Adv. Mater. **2**, 316 (1990).
[7] M. Stelze and E. Sackmann, J. Phys. Chem. **97**, 2974 (1993).
[8] A. Ottova-Leitmannova, T. Martynski, A. Wardak, and H. Tien, Self-assembling bilayer lipid membranes on solid support. Building blocks of future biosensors and molecular devices, in *Molecular Electronics*, edited by R. Birge, Vol. 240 in *Advances in Chemistry* (American Chemical Society, Washington, D.C., 1994), Chap. 17, pp. 438–454.
[9] E. Sackmann, Science **271**, 43 (1996).
[10] B. Cornell, V. Braach-Maksvytis, L. King, P. Osman, B. Raguse, L. Wieczorek, and R. Pace, Nature (London) **387**, 580 (1997).
[11] D. Dimitrov and K. Jain, Biochim. Biophys. Acta **779**, 438 (1984).
[12] J. Crowley, Biophys. J. **13**, 711 (1973).
[13] J. Weaver and Y. Chizmadzhev, Bioelectrochem. Bioenerg. **41**, 135 (1996).
[14] J. Litster, Phys. Lett. **53**, 193 (1975).
[15] I. Abidor, V. Arakelyan, L. Chernomordik, Y. A. Chizmadzhev, V. Pastushenko, and M. Tarasevich, Bioelectrochem. Bioenerg. **6**, 37 (1979).
[16] J. C. Weaver and R. Mintzer, Phys. Lett. **86A**, 57 (1981).
[17] I. Sugar, J. Physiol. (Paris) **77**, 1035 (1981).
[18] A. Vrij, Discuss. Faraday Soc. **42**, 23 (1966).
[19] A. Sheludko, Adv. Colloid Interface Sci. **1**, 391 (1967).
[20] D. Michael and M. O'Neill, J. Fluid Mech. **41**, 571 (1970).
[21] P. Bisch and H. Wendel, J. Chem. Phys. **83**, 5953 (1985).
[22] P. Bisch and H. Wendel, J. Chem. Phys. **83**, 5962 (1985).
[23] D. Dimitrov, J. Membr. Biol. **78**, 53 (1984).
[24] C. Maldarelli, R. Jain, I. Ivanov, and E. Ruckenstein, J. Colloid Interface Sci. **78**, 118 (1980).
[25] C. Maldarelli and R. Jain, J. Colloid Interface Sci. **90**, 233 (1982).
[26] C. Maldarelli and R. Jain, J. Colloid Interface Sci. **90**, 263 (1982).
[27] A. Steinchen, D. Gallez, and A. Sanfeld, J. Colloid Interface Sci. **85**, 5 (1982).
[28] D. Gallez, Biophys. Chem. **18**, 165 (1983).
[29] D. Gallez and A. Steinchen, J. Colloid Interface Sci. **94**, 296 (1983).
[30] P. Bisch, H. Wendel, and D. Gallez, J. Colloid Interface Sci. **92**, 105 (1983).
[31] D. Gallez, P. Bisch, and H. Wendel, J. Colloid Interface Sci. **92**, 121 (1983).
[32] The issue of thinning was not specifically addressed in these studies (Refs. 22,28). Attention was focused on a proper choice of the potential describing the steric interaction between the hydrocarbon tails, and the corresponding stabilization of the SQM. However, it can be shown that for

almost any choice of the quasielastic interaction stabilizing the film at low V, the critical thinning almost universally reaches 30%–40% (Ref. 50). In other words, if the potential appears softer, then V_{cr} becomes lower; however, the contraction at small voltages also becomes more extensive, so that its critical value stays approximately the same.

[33] W. Helfrich, Tension-Induced Mutual Adhesion and a Conjectured Superstructure of Lipid Membranes, in *Handbook of Biological Physics*, edited by R. Lipowsky and E. Sackmann (Elsevier Science, Washington, D.C., 1995), Vol. 1, Chap. 14, pp. 691–721.

[34] H. Huang, Biophys. J. **50**, 1061 (1986).

[35] P. Helfrich and E. Jakobsson, Biophys. J. **57**, 1075 (1990).

[36] H. Engelhart, H. Duwe, and E. Sackmann, J. Phys. (France) Lett. **46**, 395 (1985).

[37] M. B. Partenskii, V. L. Dorman, and P. C. Jordan, Biophys. J. **74**, A314 (1998).

[38] M. B. Partenskii, V. L. Dorman, and P. C. Jordan, Proc. SPIE **3253**, 266 (1998).

[39] W. Helfrich, Z. Naturforsch. C **28**, 693 (1973).

[40] S. Leikin, Biol. Membr. (Russian) **2**, 820 (1985).

[41] W. Helfrich, Z. Naturforsch. C **30**, 841 (1975).

[42] D. Andelman, Electrostatic properties of membranes: The Poisson–Boltzmann theory, in *Handbook of Biological Physics*, edited by R. Lipowsky and E. Sackmann (Elsevier Science, Washington, D.C., 1995), Vol. 1, Chap. 12, pp. 603–642.

[43] Here and in what follows we identify h_0 with the thickness of the hydrocarbon core of the lipid bilayer since the electric field is mainly confined to the low ϵ region. Alternatively we could introduce an effective thickness such that h_0/ϵ is replaced by $h_0/\epsilon+\Delta h_0/\epsilon^*$, where Δh_0 is the thickness of the head group regions and ϵ^* their mean dielectric constant. Such a modification alters estimated voltages negligibly, by $\sim$2%.

[44] D. Needham and R. Nunn, Biophys. J. **58**, 997 (1990).

[45] D. Needham and R. M. Hochmuth, Biophys. J. **55**, 1001 (1989).

[46] E. Evans and W. Rawicz, Phys. Rev. Lett. **64**, 2094 (1990).

[47] R. Benz and U. Zimmermann, Biochim. Biophys. Acta **597**, 637 (1980).

[48] G. Troiano, L. Tung, V. Sharma, and K. Stebe, Biophys. J. **75**, 880 (1998).

[49] J. Akinlaja and F. Sachs, Biophys. J. **75**, 247 (1998).

[50] M. B. Partenskii, V. Dorman, and P. C. Jordan, Int. Rev. Phys. Chem. **11**, 153 (1996).

[51] These estimates are based on direct measurements of membrane capacitance under applied voltage (Refs. 2,73–77). The following argument is also illuminating. Since the lipid is incompressible the elastic capacitor model would require significant stretching of the membrane prior to breakdown (a fractional area increase $\Delta A/A\sim 2/3$) in order to maintain constant volume. However, experimental studies of mechanical rupture indicate that the stretching preceding breakdown does not exceed 2%–5% (Refs. 2, 44, 76–79) consistent with 1%–3% thinning.

[52] As has been shown (Ref. 80), the stretching modulus that Crowley used was significantly underestimated (by almost two orders of magnitude). As a result the critical voltages that he found were well below 1 V.

[53] In the HP model it is basically assumed that the uncertainty in the values of ν is balanced by the uncertainty in the estimates of the pore formation barrier, W_{pore}, so that taken together they result in a reasonable concentration of pores. Applied voltage in this picture simply changes the concentration of pores by altering the barrier height. While an attractive picture, it requires numerous assumptions with respect to both W_{pore}, and ν_0, estimates which are difficult to verify.

[54] A. Kornyshev, Solvation of a Metal Surface, in *Chemical Physics of Solvation*, edited by R. Dogonadze, E. Kalman, A. Kornyshev, and J. Ulstrup (Elsevier Science, Amsterdam, 1985), Vol. C, Chap. 6.

[55] P. Bopp, A. Kornyshev, and G. Sutmann, J. Chem. Phys. **109**, 1939 (1998).

[56] N. Ashcroft and N. Mermin, *Solid State Physics* (Holt, Rinehart, and Winston, New York, 1977).

[57] N. Lei, C. R. Safinay, and R. Bruinsma, J. Phys. II **5**, 1155 (1993).

[58] S. Ramaswamy, J. Prost, and T. Lubensky, Europhys. Lett. **23**, 271 (1993).

[59] W. Cai, T. C. Lubensky, and T. Powers, J. Phys. II **4**, 931 (1994).

[60] S. Hladky and D. Gruen, Biophys. J. **38**, 251 (1982).

[61] J. Dilger, Biochim. Biophys. Acta **645**, 357 (1982).

[62] A. Vrij, J. Colloid Interface Sci. **51**, 1 (1964).

[63] It is more consistent to treat σ as an applied stress, because real bilayers typically attain a tensionless state (Refs. 67,68,81–85). This stress can be created either by mechanical means (e.g., osmotic stress), or by contact between the bilayer and a bulk lipid phase, due to a difference between the chemical potential of lipid in bulk and in the bilayer.

[64] W. Helfrich, Liq. Cryst. **5**, 1647 (1989).

[65] E. Sackmann, Physical basis of self-organization and function of membranes: Physics of vesicles, in *Handbook of Biological Physics*, edited by R. Lipowsky and E. Sackmann (Elsevier Science, Washington, D.C., 1995), Vol. 1, Chap. 5, pp. 213–304.

[66] J. N. Israelachvili and H. Wennerstroem, Langmuir **6**, 873 (1990).

[67] S. E. Feller and R. Pastor, Biophys. J. **71**, 1350 (1996).

[68] R. Goetz and R. Lipowsky, J. Chem. Phys. **108**, 7397 (1998).

[69] S.-W. Chiu, M. Clark, V. Balaji, S. Subramaniam, H. L. Scott, and E. Jakobsson, Biophys. J. **69**, 1230 (1995).

[70] Similar problems have been considered for various approximations and geometries for both fixed and variable membrane surface charge (Refs. 81, 86–92).

[71] W. Harrison, *Solid State Theory* (Sinauer Associates, Sunderland, MA, 1984).

[72] M. B. Partenskii and P. C. Jordan, Q. Rev. Biophys. **25**, 477 (1992).

[73] S. White and T. Thompson, Biochim. Biophys. Acta **323**, 7 (1973).

[74] O. Alvarez and R. Latorre, Biophys. J. **21**, 1 (1978).

[75] L. Chernomordik, S. Sukharev, I. Abidor, and Y. A. Chizmadzhev, Bioelectrochem. Bioenerg. **9**, 149 (1982).

[76] S. Toyama, A. Nakamura, and F. Toda, Biophys. J. **59**, 939 (1991).

[77] D. Ehrenstein and K. Iwasa, Biophys. J. **71**, 1087 (1996).

[78] E. Evans and R. Skalak, *Mechanics and Thermodynamics of Biomembranes* (CRC Press, Florida, 1980).

[79] E. Evans and D. Needham, J. Phys. Chem. **91**, 4219 (1987).

[80] J. Requena, D. A. Haydon, and S. Hladky, Biophys. J. **15**, 77 (1975).

[81] D. Bensimon, F. David, S. Leibler, and A. Pumir, J. Phys. France **51**, 689 (1990).

[82] M. Bloom, E. Evans, and O. Mouritsen, Q. Rev. Biophys. **24**, 293 (1991).

[83] D. Sornette and N. Ostrowsky, Lamellar Phases: Effect of Fluctuations (Theory), in *Micelles, Membranes, Microemulsions, and Monolayers*, edited by W. Gelbart, A. Ben-Shaul, and D. Roux (Springer, New York, 1994), Chap. 5, pp. 251–302.

[84] D. Marsh, Biochim. Biophys. Acta **1286**, 183 (1996).

[85] F. Jahning, Biophys. J. **71**, 1348 (1996).

[86] M. Winterhalter and W. Helfrich, J. Phys. Chem. **92**, 6865 (1988).

[87] D. Mitchell and B. Ninham, Langmuir **5**, 1121 (1989).

[88] A. Fogden, D. Mitchell, and B. Ninham, Langmuir **6**, 159 (1990).

[89] A. Fogden and B. Ninham, Langmuir **7**, 590 (1991).

[90] M. Winterhalter and W. Helfrich, J. Phys. Chem. **96**, 327 (1992).

[91] M. Winterhalter, Prog. Colloid Polym. Sci. **98**, 271 (1995).

[92] S. May, J. Chem. Phys. **105**, 8314 (1996).